

# The transfer of resonance line polarization with partial frequency redistribution in the general Hanle-Zeeman regime

E. Alsina Ballester<sup>1,2</sup>, L. Belluzzi<sup>3,4</sup>, and J. Trujillo Bueno<sup>1,2,5</sup>

ealsina@iac.es

## ABSTRACT

The spectral line polarization encodes a wealth of information about the thermal and magnetic properties of the solar atmosphere. Modeling the Stokes profiles of strong resonance lines is, however, a complex problem both from the theoretical and computational point of view, especially when partial frequency redistribution (PRD) effects need to be taken into account. In this work, we consider a two-level atom in the presence of magnetic fields of arbitrary intensity (Hanle-Zeeman regime) and orientation, both deterministic and micro-structured. Working within the framework of a rigorous PRD theoretical approach, we have developed a numerical code which solves the full non-LTE radiative transfer problem for polarized radiation, in one-dimensional models of the solar atmosphere, accounting for the combined action of the Hanle and Zeeman effects, as well as for PRD phenomena. After briefly discussing the relevant equations, we describe the iterative method of solution of the problem and the numerical tools that we have developed and implemented. We finally present some illustrative applications to two resonance lines that form at different heights in the solar atmosphere, and provide a detailed physical interpretation of the calculated Stokes profiles. We find that in strong resonance lines sensitive to PRD effects the magneto-optical  $\rho_V$  terms of the Stokes-vector transfer equation produce conspicuous  $U/I$  wing signals along with a very interesting magnetic sensitivity in the wings of the linear polarization profiles. We also show that the weak-field approximation has to be used with caution when PRD effects are considered.

*Subject headings:* line: profiles — polarization — radiative transfer — methods: numerical — Sun: atmosphere — stars: atmospheres

---

<sup>1</sup>Instituto de Astrofísica de Canarias, E-38205 La Laguna, Tenerife, Spain

<sup>2</sup>Departamento de Astrofísica, Facultad de Física, Universidad de La Laguna, Tenerife, Spain

<sup>3</sup>Istituto Ricerche Solari Locarno, CH-6605 Locarno Monti, Switzerland

<sup>4</sup>Kiepenheuer-Institut für Sonnenphysik, D-79104 Freiburg, Germany

<sup>5</sup>Consejo Superior de Investigaciones Científicas, Spain

## 1. Introduction

The most important physical observable for probing the thermal, dynamic, and magnetic properties of stellar atmospheres is the emerging radiation. Aside from its intensity, the radiation is characterized by a given polarization state, which contains crucial information about the magnetic fields present in the atmosphere. Although the magnetic field is known to play a key role in the atmosphere of the Sun and other stars, our empirical knowledge of its intensity and orientation is still largely unsatisfactory, and basically limited to the deepest layers (the photosphere). This explains the importance of developing new techniques for magnetic field diagnostics, based on the accurate measurement and interpretation of the polarization properties of the radiation field. Each line of the solar spectrum gives information on the physical properties of the solar atmosphere at a certain height range, depending on the opacity of the atmosphere at the frequency of the line in question. As examples, the Sr I line at 4607 Å can be used to obtain information on the Sun’s photosphere (e.g., Trujillo Bueno et al. 2004), while the lower chromosphere can be studied via the Sr II line at 4078 Å (e.g., Bianda et al. 1998). Interpreting these Stokes profiles requires solving a radiative transfer problem out of local thermodynamic equilibrium (non-LTE), which becomes more complex if, besides the well-known Zeeman effect, we wish to model the impact of scattering polarization and its modification due to the presence of a magnetic field (Hanle effect).

A solid theory for the generation and transfer of polarized radiation, based on a first-order perturbative expansion of the atom-radiation interaction within the framework of quantum electrodynamics, is today available (e.g., Landi Degl’Innocenti & Landolfi 2004, hereafter LL04). Within this theory, the scattering of a photon, which is intrinsically a second-order process, is described as a temporal succession of independent absorption and re-emission processes (Markov approximation). This case, generally referred to as the limit of complete frequency redistribution (CRD) is strictly correct either when collisions are extremely efficient in relaxing any possible correlation between the frequencies of the incoming and outgoing photons, or when the pumping field is spectrally flat (e.g., Casini & Landi Degl’Innocenti 2007). Nonetheless, it can be shown that even when the above-mentioned conditions are not strictly verified, the limit of CRD represents in any case a suitable approximation for modeling the center of the spectral lines, where the Hanle effect takes place. This theory, on the other hand, turns out to be unsuitable to model the wings of strong spectral lines, where coherent scattering and partial frequency redistribution (PRD) effects play a fundamental role. Different theoretical approaches suitable to describe coherent scattering processes have been proposed during the last years.<sup>1</sup> One is based on the Kramers-Heisenberg scattering formula. This approach was initially proposed by Stenflo (1994), and it has been recently extended to increasingly complex atomic models in the presence of arbitrary magnetic fields (e.g., Sowmya et al. 2014, 2015).

---

<sup>1</sup> By “coherent scattering” we mean here a scattering process in which the frequencies of the absorbed and emitted photons are either identical (if the initial and final states coincide), or satisfy the Raman scattering rule (if the initial and final states differ). In this sense, coherent scattering is strictly valid in the atomic reference frame, when the atom does not interact with any other particle (collisionless regime), and when the lower level can be assumed to be infinitely sharp (which is generally a good approximation when this is either the ground or a metastable level).

Another approach, also suitable to describe complex atomic models in the presence of arbitrary magnetic fields, is based on the heuristic idea of metalevels (see Landi Degl’Innocenti et al. 1997). A new quantum mechanical approach, capable of considering higher-order processes through a diagrammatic treatment of the atom-radiation interaction, has been recently proposed by Casini et al. (2014).

The coherency of scattering can be relaxed through two different physical mechanisms: the Doppler effect and collisional processes. Doppler redistribution must always be considered when going from the atomic frame to the observer’s one. Its inclusion in the above-mentioned approaches does not present particular difficulties from the theoretical point of view, although it leads to rather complex mathematical expressions. On the contrary, the generalization of these approaches so to include collisional processes is not trivial, and it is still under investigation. A theoretical approach based on a perturbative expansion of the atom-radiation interaction, which includes collisional redistribution, has been proposed by Bommier (1997a,b) for the case of a two-level atom. This approach, which is based on the redistribution matrix formalism, is the starting point of our work. We consider a two-level model atom with an unpolarized and infinitely sharp lower level. This atomic model is not only of academic interest, but is suitable to model various strong resonance lines of diagnostic relevance, such as the Sr I line at 4607 Å, or the Ca I line at 4227 Å. Indeed, we observe that the lower levels of these lines, having total angular momenta  $J = 1/2$  and  $J = 0$ , respectively, cannot be polarized (in particular, they cannot carry atomic alignment) by definition<sup>2</sup>. Moreover, these levels are the ground levels of the corresponding atomic species, so that the assumption that they are infinitely sharp is a very good approximation.

In this work the solar atmosphere is modeled as one-dimensional, static, and plane-parallel. Though considering the atmosphere as dynamic and three-dimensional is a much more realistic treatment for the generation and transfer of polarized radiation, the approach presented here is a suitable first step, in which much faster calculations can be performed, yielding many insights into the physical mechanisms involved.

In Sect. 2, we present the starting equations, written in the atomic reference frame, with the quantization axis directed along the magnetic field, and we discuss their transformation into an arbitrary reference frame. Obtaining the emergent intensity and polarization requires finding the self-consistent solution of the statistical equilibrium (SE) equations for the atomic state, and of the radiative transfer (RT) equations.<sup>3</sup> This is done through an iterative method that is described in Sect. 3, together with the numerical tools that have been developed and implemented, considering the particular characteristics of the problem under investigation. When PRD phenomena are taken

---

<sup>2</sup>Note that levels with  $J = 1/2$  can be polarized (they can carry atomic orientation) if the incident radiation is circularly polarized. In this work, we assume that collisional depolarization is always sufficiently strong so to destroy any atomic orientation that might be induced in the (long-lived) lower level of these resonance lines

<sup>3</sup> This investigation is carried out within the framework of the redistribution matrix formalism. We recall that the redistribution matrix is based on an analytical solution of the SE equations, which therefore do not explicitly appear in the problem, when this formalism is applied.

into account, the emitted radiation at a given frequency does not depend only on the incoming radiation at that specific frequency (as would happen for coherent scattering), nor does it depend on a frequency-averaged radiation field (as in CRD). In consequence, the iterative scheme has to consider that all frequencies are coupled to one another in the scattering process. The possibility of having a magnetic field which is micro-structured, and its effect in this radiative transfer problem is discussed in Sect. 4. In Sect. 5 we present some illustrative applications to some lines of diagnostic interest, based on the theory and numerical methods discussed in this paper.

## 2. Formulation of the problem

In this work we consider a two-level atom with an unpolarized and infinitely-sharp lower level. The general RT equation that we need to solve in order to find the polarized radiation emerging from a stellar atmosphere can be written as

$$\frac{d}{ds} \begin{pmatrix} I \\ Q \\ U \\ V \end{pmatrix} = \begin{pmatrix} \varepsilon_I \\ \varepsilon_Q \\ \varepsilon_U \\ \varepsilon_V \end{pmatrix} - \begin{pmatrix} \eta_I & \eta_Q & \eta_U & \eta_V \\ \eta_Q & \eta_I & \rho_V & -\rho_U \\ \eta_U & -\rho_V & \eta_I & \rho_Q \\ \eta_V & \rho_U & -\rho_Q & \eta_I \end{pmatrix} \begin{pmatrix} I \\ Q \\ U \\ V \end{pmatrix} \quad (1)$$

where  $I$ ,  $Q$ ,  $U$ , and  $V$  are the four Stokes parameters, and  $s$  is the spatial coordinate along the ray path. The quantities  $\varepsilon_X$  ( $X = I, Q, U$ , and  $V$ ) are the emission coefficients in the four Stokes parameters, the coefficients  $\eta_X$  describe the differential absorption of the various polarization states (dichroism), while the coefficients  $\rho_X$  describe couplings between different Stokes parameters (anomalous dispersion effects). As is well known, stimulated emission is negligible in the solar atmosphere, and so will not be taken into account in this work. The Stokes parameters and the RT coefficients are in general functions of the spatial point, and of the frequency ( $\nu$ ) and propagation direction ( $\vec{\Omega}$ ) of the radiation beam under consideration. The RT coefficients depend on the state of the atoms that, in non-LTE conditions, has to be calculated by solving the SE equations. When polarization phenomena are considered, it is necessary to provide a complete description of the atomic state, by specifying the population of the various magnetic sublevels as well as the quantum interference (or coherence) that may be present between pairs of them. Whenever the magnetic sublevels are not evenly populated and/or quantum interference between pairs of them is present, the atomic level is said to be polarized. In general, the four Stokes parameters are coupled to one another, and we solve the transfer equation numerically, by applying a short-characteristics method known as DELOPAR (see Trujillo Bueno 2003).

In general, the RT coefficients appearing in Eq. (1) contain contributions due to both line and continuum processes. Hereafter, the line and continuum contributions will be distinguished through the labels  $\ell$  and  $c$ , respectively. Observing that dichroism and anomalous dispersion effects are generally negligible in the continuum spectrum, we have

$$\eta_i^c(\nu) = \delta_{i0} \eta_I^c(\nu), \quad (2)$$

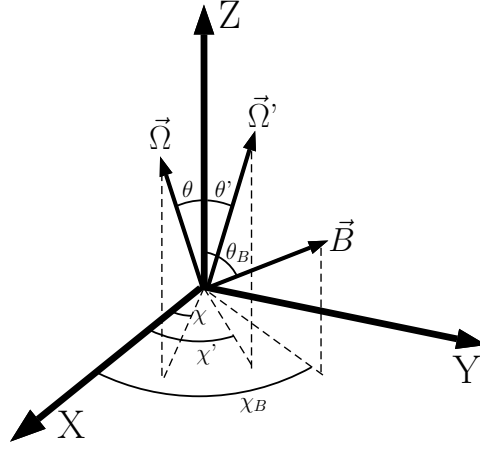


Fig. 1.— Geometry of the problem. We take a right-handed Cartesian coordinate system with the Z-axis (quantization axis for the angular momentum) along the local vertical, and the X-axis directed so that the line of sight towards the observer lies in the X-Z plane. In this reference system, the direction of the magnetic field  $\vec{B}$  is specified by its inclination with respect to the vertical ( $\theta_B$ ) and its azimuth ( $\chi_B$ ). Similarly, the direction of the incoming photon ( $\vec{\Omega}'$ ) is specified by the angles ( $\theta', \chi'$ ) and for the outgoing photon the direction ( $\vec{\Omega}$ ) is specified by angles ( $\theta, \chi$ )

with  $i = 0, 1, 2$ , and  $3$ , standing for Stokes  $I$ ,  $Q$ ,  $U$ , and  $V$ , respectively, and

$$\rho_i^c(\nu) = 0, \quad (i = 1, 2, 3). \quad (3)$$

It is worth noting that the continuum contribution to  $\eta_I$  has a frequency dependence, but is independent of the direction of propagation of the radiation. Considering the contributions to the continuum due to both scattering processes, which we assume to be coherent, and thermal processes, the emission coefficient is given by (see LL04):

$$\varepsilon_i^c(\nu, \vec{\Omega}) = \sigma(\nu) \sum_{KQ} \mathcal{T}_Q^K(i, \vec{\Omega}) (-1)^Q J_{-Q}^K(\nu) + \varepsilon_{th}(\nu) \delta_{i0}. \quad (4)$$

where  $\sigma(\nu)$  is the continuum scattering cross section and  $\varepsilon_{th}(\nu)$  is the thermal continuum emission coefficient. The quantity  $\mathcal{T}_Q^K(i, \vec{\Omega})$  is the so-called polarization tensor (see Sect. 5.11 of LL04), an irreducible spherical tensor of rank  $K = 0, 1, 2$  ( $Q$  is an integer ranging from  $-K$  to  $K$ ). The radiation field tensor,  $J_Q^K(\nu)$ , which provides a complete description of the symmetry properties of the radiation field, is defined by

$$J_Q^K(\nu) = \oint \frac{d\vec{\Omega}}{4\pi} \sum_{j=0}^3 \mathcal{T}_Q^K(j, \vec{\Omega}) I_j(\nu, \vec{\Omega}), \quad (5)$$

where  $I_j(\nu, \vec{\Omega})$  is the Stokes vector (i.e., a vector whose components are the four Stokes parameters).

The line contributions to  $\eta_i$  and  $\rho_i$  are calculated according to LL04. For the particular case of a two-level atom with an unpolarized lower level, in the atomic rest frame, and taking the quantization axis for the angular momentum along the direction of the magnetic field we have

$$\eta_i^\ell(\nu, \vec{\Omega}) = k_L \sum_K \Phi_0^{0K}(J_\ell, J_u; \nu) \mathcal{T}_0^K(i, \vec{\Omega}), \quad (6a)$$

$$\rho_i^\ell(\nu, \vec{\Omega}) = k_L \sum_K \Psi_0^{0K}(J_\ell, J_u; \nu) \mathcal{T}_0^K(i, \vec{\Omega}), \quad (6b)$$

where  $k_L$  is the frequency-integrated absorption coefficient, defined by

$$k_L = \frac{h\nu}{4\pi} \mathcal{N}_\ell B_{\ell u}, \quad (7)$$

where  $h$  is the Planck constant,  $\mathcal{N}_\ell$  is the population of the lower level, and  $B_{\ell u}$  is the Einstein coefficient for absorption. The quantities  $\Phi_Q^{KK'}(J_\ell, J_u; \nu)$  and  $\Psi_Q^{KK'}(J_\ell, J_u; \nu)$  are the so-called generalized profile and generalized dispersion profile, respectively, defined as:

$$\begin{aligned} \Phi_Q^{KK'}(J_\ell, J_u; \nu) &= \sqrt{3(2J_u + 1)(2K + 1)(2K' + 1)} \\ &\times \sum_{M_u M_u' M_\ell q q'} (-1)^{1+J_u-M_u+q'} \begin{pmatrix} J_u & J_\ell & 1 \\ -M_u & M_\ell & -q \end{pmatrix} \begin{pmatrix} J_u & J_\ell & 1 \\ -M_u' & M_\ell & -q' \end{pmatrix} \\ &\times \begin{pmatrix} J_u & J_u & K \\ M_u' & -M_u & -Q \end{pmatrix} \begin{pmatrix} 1 & 1 & K' \\ q & -q' & -Q \end{pmatrix} \frac{1}{2} \left[ \Phi(\nu_{M_u M_\ell} - \nu) + \Phi(\nu_{M_u' M_\ell} - \nu) \right], \end{aligned} \quad (8)$$

and

$$\begin{aligned} \Psi_Q^{KK'}(J_\ell, J_u; \nu) &= \sqrt{3(2J_u + 1)(2K + 1)(2K' + 1)} \\ &\times \sum_{M_u M_u' M_\ell q q'} (-1)^{1+J_u-M_u+q'} \begin{pmatrix} J_u & J_\ell & 1 \\ -M_u & M_\ell & -q \end{pmatrix} \begin{pmatrix} J_u & J_\ell & 1 \\ -M_u' & M_\ell & -q' \end{pmatrix} \\ &\times \begin{pmatrix} J_u & J_u & K \\ M_u' & -M_u & -Q \end{pmatrix} \begin{pmatrix} 1 & 1 & K' \\ q & -q' & -Q \end{pmatrix} \frac{(-i)}{2} \left[ \Phi(\nu_{M_u M_\ell} - \nu) - \Phi(\nu_{M_u' M_\ell} - \nu)^* \right], \end{aligned} \quad (9)$$

where  $J_u$  and  $J_\ell$  are the total angular momenta of the upper and lower level, respectively, while  $M_u$  and  $M_\ell$  are the magnetic quantum numbers for the Zeeman sublevels of the upper and lower level, respectively. The frequencies  $\nu_{M_u M_\ell}$  are defined as

$$\nu_{M_u M_\ell} = \frac{E(M_u) - E(M_\ell)}{h},$$

where  $E(M_u)$  and  $E(M_\ell)$  are the energies of the magnetic sublevels  $M_u$  and  $M_\ell$ , respectively. The indices can take the following values

$$\begin{aligned} K &= 0, 1, \dots, 2J_u, \\ K' &= 0, 1, 2, \end{aligned} \quad (10)$$

$$Q = 0, \pm 1, \pm 2, \quad |Q| \leq K, \quad |Q| \leq K'.$$

The  $\Phi$  profiles are defined by

$$\Phi(\nu_0 - \nu) = \phi(\nu_0 - \nu) + i\psi(\nu_0 - \nu),$$

where, in the atomic reference frame,  $\phi(\nu_0 - \nu)$  is the Lorentzian profile and  $\psi(\nu_0 - \nu)$  the associated dispersion profile.

Working within the framework of the redistribution matrix formalism, the line part of the emission coefficient is given by

$$\begin{aligned} \varepsilon_i^\ell(\nu, \vec{\Omega}) = & k_L \int_0^\infty d\nu' \oint \frac{d\vec{\Omega}'}{4\pi} \sum_{j=0}^3 \left[ \mathcal{R}(\nu', \vec{\Omega}', \nu, \vec{\Omega}; \vec{B}) \right]_{ij} I_j(\nu', \vec{\Omega}') \\ & + k_L \frac{\epsilon'}{1 + \epsilon'} B_T(\nu_0) \sum_K \mathcal{T}_0^K(i, \vec{\Omega}) \Phi_0^{0K}(J_\ell, J_u; \nu). \end{aligned} \quad (11)$$

The second term in the right-hand side of Eq. (11), generally referred to as the collisional (or thermal) term, describes the contribution to the emission coefficient due to atoms excited by isotropic collisions. This term depends on the parameter  $\epsilon' = C_{ul}/A_{ul}$ , with  $C_{ul}$  the inelastic collisional de-excitation rate and  $A_{ul}$  the Einstein coefficient for spontaneous emission. The quantity  $B_T(\nu_0)$  is the Planck function in the Wien limit (consistently with our assumption of neglecting stimulated emission) at the line-center frequency  $\nu_0$ , and at the temperature  $T$ . The radiative part of the emission coefficient (first term in the righthand side of Eq. 11) contains the redistribution matrix  $[\mathcal{R}(\nu', \vec{\Omega}', \nu, \vec{\Omega}; \vec{B})]_{ij}$ , where the primed quantities refer to the incoming radiation, while the unprimed ones refer to the outgoing radiation. The redistribution matrix allows us to relate the emission coefficient directly to the Stokes parameters of the incoming radiation, a circumstance that is only possible when an analytical solution of the SE equations is available. It can be shown that the most general form of the redistribution matrix is given by the linear combination of two terms, one describing purely coherent scattering (CS) in the atomic rest frame, and one describing scattering processes in the limit of CRD (following the terminology introduced by Hummer (1962) these redistribution matrices are generally indicated with the symbols  $\mathcal{R}_{\text{II}}$  and  $\mathcal{R}_{\text{III}}$ , respectively):

$$\left[ \mathcal{R}(\nu', \vec{\Omega}', \nu, \vec{\Omega}; \vec{B}) \right]_{ij} = \left[ \mathcal{R}_{\text{II}}(\nu', \vec{\Omega}', \nu, \vec{\Omega}; \vec{B}) \right]_{ij} + \left[ \mathcal{R}_{\text{III}}(\nu', \vec{\Omega}', \nu, \vec{\Omega}; \vec{B}) \right]_{ij}, \quad (12)$$

The details of the atom-radiation interaction, and therefore the relevant physics of partial frequency redistribution phenomena, are contained in the redistribution matrix. In this work, we consider the redistribution matrix derived by Bommier (1997a,b) for the case of a two-level atom with unpolarized and infinitely-sharp lower level, in the presence of arbitrary magnetic fields. This redistribution matrix accounts for the various effects of elastic collisions, namely, level broadening, relaxation of atomic polarization, and frequency redistribution in the scattering processes. We

observe that the assumption of infinitely-sharp lower level is valid whenever the lifetime of the lower level is very large, and therefore is perfectly suitable for resonance lines, since their lower level is, by definition, the ground level. In the atomic rest frame, and taking the quantization axis along the magnetic field, the  $\mathcal{R}_{\text{II}}$  and  $\mathcal{R}_{\text{III}}$  redistribution matrices derived by Bommier (1997b) have the following expressions:<sup>4</sup>

$$\begin{aligned} \left[ \mathcal{R}_{\text{II}}(\nu', \vec{\Omega}', \nu, \vec{\Omega}; \vec{B}) \right]_{ij} = & \sum_{K'K''Q} \sum_{M_u M_u' M_\ell M_\ell'} \mathcal{C}_{K'K''Q M_u M_u' M_\ell M_\ell' p p' p'' p'''} \frac{\Gamma_R}{\Gamma_R + \Gamma_I + \Gamma_E + i\omega_L g_{J_u} Q} \\ & \times (-1)^Q \mathcal{T}_Q^{K''}(i, \vec{\Omega}) \mathcal{T}_{-Q}^{K'}(j, \vec{\Omega}') \delta(\nu - \nu' - \nu_{M_\ell M_\ell'}) \frac{1}{2} \left[ \Phi(\nu_{M_u' M_\ell} - \nu') + \Phi^*(\nu_{M_u M_\ell} - \nu') \right], \end{aligned} \quad (13)$$

$$\begin{aligned} \left[ \mathcal{R}_{\text{III}}(\nu', \vec{\Omega}', \nu, \vec{\Omega}; \vec{B}) \right]_{ij} = & \sum_{KK'K''Q} \left[ \frac{\Gamma_R}{\Gamma_R + \Gamma_I + D^{(K)} + i\omega_L g_u Q} - \frac{\Gamma_R}{\Gamma_R + \Gamma_I + \Gamma_E + i\omega_L g_u Q} \right] \\ & \times (-1)^Q \mathcal{T}_Q^{K''}(i, \vec{\Omega}) \mathcal{T}_{-Q}^{K'}(j, \vec{\Omega}') \Phi_Q^{KK''}(J_\ell, J_u; \nu) \Phi_Q^{KK'}(J_\ell, J_u; \nu'), \end{aligned} \quad (14)$$

where  $\Gamma_R$ ,  $\Gamma_I$  and  $\Gamma_E$  are the line broadening constants for radiative decays, collisional de-excitation and elastic collisions respectively:

$$\Gamma_R = A_{u\ell}, \quad \Gamma_I = C_{u\ell}, \quad \Gamma_E = Q_{\text{el}},$$

with  $Q_{\text{el}}$  the elastic collision rate. The rate  $D^{(K)}$  is the  $K$ -multipole component of the depolarizing rate due to elastic collisions,  $\omega_L$  is the angular Larmor frequency, and  $g_u$  is the Landé factor of the upper level. The quantity  $\mathcal{C}_{K'K''Q M_u M_u' M_\ell M_\ell' p p' p'' p'''}$  is a real number which depends on the indices and quantum numbers indicated as pedices. Its explicit expression is given by (see Bommier 1997b)

$$\begin{aligned} \mathcal{C}_{K'K''Q M_u M_u' M_\ell M_\ell' p p' p'' p'''} = & 3(2J_u + 1) \sqrt{2K' + 1} \sqrt{2K'' + 1} (-1)^{2J_u - M_\ell - M_\ell'} \\ & \times \begin{pmatrix} J_u & J_\ell & 1 \\ M_u & -M_\ell & -p \end{pmatrix} \begin{pmatrix} J_u & J_\ell & 1 \\ M_u' & -M_\ell & -p' \end{pmatrix} \begin{pmatrix} J_u & J_\ell & 1 \\ M_u & -M_\ell' & -p'' \end{pmatrix} \\ & \times \begin{pmatrix} J_u & J_\ell & 1 \\ M_u' & -M_\ell' & -p''' \end{pmatrix} \begin{pmatrix} 1 & 1 & K' \\ -p & p' & Q \end{pmatrix} \begin{pmatrix} 1 & 1 & K'' \\ -p'' & p''' & Q \end{pmatrix}. \end{aligned} \quad (15)$$

---

<sup>4</sup>The approximation  $\nu/\nu_0 \approx 1$  has been used, which is valid because, at frequencies significantly different from  $\nu_0$ ,  $\varepsilon_i^\ell(\nu, \vec{\Omega}) \rightarrow 0$ .



## 2.1. Expressions in an arbitrary reference frame

The previous expressions for the redistribution matrices are given in the magnetic reference frame, i.e., the frame in which the quantization axis is parallel to the direction of the magnetic field. However, one may want to express them in an arbitrary, fixed reference frame, by changing the direction of the quantization axis (e.g., taking it along the vertical direction for a plane-parallel atmosphere). This transformation can be performed as described in Sect. 7.12 of LL04, taking into account the following rotation rule of the polarization tensor

$$\mathcal{T}_{Q'}^K(i, \vec{\Omega}) \Big|_{\text{new}} = \sum_Q \mathcal{T}_Q^K(i, \vec{\Omega}) \Big|_B \mathcal{D}_{QQ'}^K(R_B), \quad (16)$$

and the inverse relation

$$\mathcal{T}_{Q'}^K(i, \vec{\Omega}) \Big|_B = \sum_Q \mathcal{T}_Q^K(i, \vec{\Omega}) \Big|_{\text{new}} \mathcal{D}_{Q'Q}^K(R_B)^*, \quad (17)$$

with  $\mathcal{D}_{QQ'}^K(R_B)$  the rotation matrix, and  $R_B$  the rotation that brings the magnetic reference frame into the new reference frame. For an arbitrary rotation  $R = (\alpha, \beta, \gamma)$ , with  $\alpha$ ,  $\beta$  and  $\gamma$  the Euler angles, the rotation matrix  $\mathcal{D}_{Q_1 Q_2}^K(R)$  is given by

$$\mathcal{D}_{Q_1 Q_2}^K(R) = \exp \left[ i(\alpha Q_1 + \gamma Q_2) \right] d_{Q_1 Q_2}^K(\beta), \quad (18)$$

where  $d_{Q_1 Q_2}^K(\beta)$  is the so-called reduced rotation matrix, which is a real number that contains the information on the change in inclination of the system due to the rotation. Referring to Fig. 1, the rotation  $R_B$  is defined by the Euler angles  $R_B = (0, -\theta_B, -\chi_B)$ .<sup>5</sup>

Using Eqs. (16) and (17), we can easily find the expressions of  $\eta_i(\nu, \vec{\Omega})$ ,  $\rho_i(\nu, \vec{\Omega})$ , and  $\varepsilon_i(\nu, \vec{\Omega})$  (for both line and continuum processes) in an arbitrary reference frame. In particular, in the new reference frame, the redistribution matrices take the form:

$$\begin{aligned} \left[ \mathcal{R}_{\text{II}}(\nu', \vec{\Omega}', \nu, \vec{\Omega}; \vec{B}) \right]_{ij} = & \sum_{K'K''Q'Q''} \sum_{\substack{M_u' M_u M_\ell' M_\ell \\ pp'p''p'''}} \mathcal{C}_{K'K''QM_u M_u' M_\ell M_\ell' pp'p''p'''} \frac{\Gamma_R}{\Gamma_R + \Gamma_I + \Gamma_E + i\omega_L g_u \bar{Q}} \\ & \times (-1)^{Q'} \mathcal{T}_{Q''}^{K''}(i, \vec{\Omega}) \mathcal{T}_{-Q'}^{K'}(j, \vec{\Omega}') \mathcal{D}_{Q'Q''}^{K'}(R_B) \mathcal{D}_{Q'Q''}^{K''}(R_B) \\ & \times \delta(\nu - \nu' - \nu_{M_\ell' M_\ell}) \frac{1}{2} \left[ \Phi(\nu_{M_u' M_\ell} - \nu') + \Phi(\nu_{M_u M_\ell} - \nu')^* \right]. \end{aligned} \quad (19)$$

---

<sup>5</sup>In full generality, there would be a third Euler angle  $\alpha_B$ . Nonetheless, it can be proven that for the problem under consideration, the expressions of the rotation matrices are independent of the choice of  $\alpha_B$ , which can thus be chosen to be zero.

$$\begin{aligned}
\left[ \mathcal{R}_{\text{III}}(\nu', \vec{\Omega}, \nu, \vec{\Omega}; \vec{B}) \right]_{ij} = & \\
\sum_{KK'K''QQ'Q''} & \left[ \frac{\Gamma_R}{\Gamma_R + \Gamma_I + D^{(K)} + i\omega_L g_u Q} - \frac{\Gamma_R}{\Gamma_R + \Gamma_I + \Gamma_E + i\omega_L g_u Q} \right] \\
& \times (-1)^{Q'} \mathcal{T}_{Q''}^{K''}(i, \vec{\Omega}) \mathcal{T}_{-Q'}^{K'}(j, \vec{\Omega}') \mathcal{D}_{QQ'}^{K'}(R_B) \mathcal{D}_{QQ''}^{K''}(R_B)^* \\
& \times \Phi_Q^{KK''}(J_\ell, J_u; \nu) \Phi_Q^{KK'}(J_\ell, J_u; \nu').
\end{aligned} \tag{20}$$

Now it is useful to factorize the redistribution matrices as follows

$$\left[ \mathcal{R}_X(\nu', \vec{\Omega}', \nu, \vec{\Omega}; \vec{B}) \right]_{ij} = \sum_{K'K''Q} [R_X]_Q^{K'K''}(\nu', \nu, B) \left[ \mathcal{P}_Q^{K'K''}(\vec{\Omega}', \vec{\Omega}, \hat{b}) \right]_{ij}, \tag{21}$$

with  $X = \text{II}, \text{III}$ , and where the magnetic field has been indicated as  $\vec{B} = B\hat{b}$ . In this way, all the dependence of the redistribution matrix on the geometrical part of the problem (i.e., propagation directions of the incoming and outgoing radiation, and the orientation of the magnetic field) is contained in the scattering phase matrix

$$\left[ \mathcal{P}_Q^{K'K''}(\vec{\Omega}', \vec{\Omega}, \hat{b}) \right]_{ij} = \sum_{Q'Q''} (-1)^{Q'} \mathcal{T}_{Q''}^{K''}(i, \vec{\Omega}) \mathcal{T}_{-Q'}^{K'}(j, \vec{\Omega}') \mathcal{D}_{QQ'}^{K'}(R_B) \mathcal{D}_{QQ''}^{K''}(R_B)^*. \tag{22}$$

## 2.2. Expressions in the observer's frame

The expressions derived in the previous section are still valid in the atom's reference frame. We discuss now the transformation into the observer's frame, where Doppler redistribution has to be taken into account. The Doppler effect only affects the frequency-dependent part of the redistribution matrix, the scattering phase matrix remaining unchanged. Assuming that the atoms have a Maxwellian distribution for both the thermal and microturbulent velocities, following Mihalas (1978), we find for  $R_{\text{II}}$

$$\begin{aligned}
[R_{\text{II}}^{\text{obs}}]_Q^{K'K''}(\nu', \nu, \Theta, B) = & \\
\sum_{\substack{M_u M_u' M_\ell M_\ell' \\ pp'p''p'''}} & \mathcal{C}_{K'K''QM_u M_u' M_\ell M_\ell' pp'p''p'''} \frac{\Gamma_R}{\Gamma_R + \Gamma_I + \Gamma_E + i\omega_L g_{J_u} Q} \\
& \times \frac{1}{\pi \Delta \nu_D^2} \frac{1}{\sin \Theta} \exp \left[ - \left( \frac{\nu' - \nu + \nu_{M_\ell M_\ell'}}{2 \Delta \nu_D \sin(\Theta/2)} \right)^2 \right] \\
& \times \frac{1}{2} \left[ W \left( \frac{a}{\cos(\Theta/2)}, \frac{x_{M_u' M_\ell} + x'_{M_u' M_\ell'}}{2 \cos(\Theta/2)} \right) + W \left( \frac{a}{\cos(\Theta/2)}, \frac{x_{M_u M_\ell} + x'_{M_u M_\ell'}}{2 \cos(\Theta/2)} \right)^* \right],
\end{aligned} \tag{23}$$

where  $\Theta$  is the scattering angle (i.e., the angle between the directions of the incoming and outgoing photons), and where the function  $W$  is defined by:

$$W(a, x) = H(a, x) + i L(a, x), \tag{24}$$

with  $H$  the Voigt function, and  $L$  the Faraday-Voigt dispersion profile. The quantity  $a = \Gamma/4\pi\Delta\nu_D$  is the damping parameter, with  $\Gamma = \Gamma_R + \Gamma_I + \Gamma_E$ . The reduced frequencies are defined as:

$$x_{M_u M_\ell} = \frac{\nu_{M_u M_\ell} - \nu}{\Delta\nu_D}, \quad x'_{M_u M_\ell} = \frac{\nu_{M_u M_\ell} - \nu'}{\Delta\nu_D}. \quad (25)$$

Because of the presence of the angle  $\Theta$  in the quantity  $[R_{\text{II}}^{\text{obs}}]_Q^{K'K''}(\nu', \nu, \Theta, B)$ , the angular and frequency dependencies cannot be factorized (as could be done in the atomic rest frame), which makes the problem significantly more complicated from the numerical point of view. In order to simplify it, we follow Rees & Saliba (1982), and we consider the expression of  $[R_{\text{II}}^{\text{obs}}]_Q^{K'K''}$  averaged over the scattering angle (angle-averaged approximation). Detailed information on the range of validity of this approximation can be found in Faurobert (1987, 1988) in the absence of magnetic field. For a discussion of the validity of this approximation in the presence of a weak magnetic field see Sampoorana et al. (2008) and Sampoorana (2011). Using such approximation, the frequency-dependent part of the redistribution function becomes:

$$\begin{aligned} [R_{\text{II-AA}}^{\text{obs}}]_Q^{K'K''}(\nu', \nu; B) = & \sum_{\substack{M_u M_u' M_\ell M_\ell' \\ pp'p''p'''}} \mathcal{C}_{K'K''QM_u M_u' M_\ell M_\ell' pp'p''p'''} \frac{\Gamma_R}{\Gamma_R + \Gamma_I + \Gamma_E + i\omega_L g_{J_u} Q} \\ & \times \frac{1}{2\pi\Delta\nu_D^2} \int_0^\pi d\Theta \exp \left[ - \left( \frac{\nu' - \nu + \nu_{M_\ell M_\ell'}}{2\Delta\nu_D \sin(\Theta/2)} \right)^2 \right] \\ & \times \frac{1}{2} \left[ W \left( \frac{a}{\cos(\Theta/2)}, \frac{x_{M_u' M_\ell} + x'_{M_u' M_\ell'}}{2 \cos(\Theta/2)} \right) + W \left( \frac{a}{\cos(\Theta/2)}, \frac{x_{M_u M_\ell} + x'_{M_u M_\ell'}}{2 \cos(\Theta/2)} \right)^* \right]. \end{aligned} \quad (26)$$

The integration over the scattering angle  $\Theta$  is performed numerically, using a Gauss-Legendre quadrature rule.<sup>6</sup> The dependence on this angle is contained in the exponential and  $W$  functions, both of which become steeper as their arguments approach zero. For this reason, the number of quadrature points has been chosen depending on the considered frequencies of the incoming and outgoing photons. A particularly high number of points (of the order of 100) has to be considered when the frequencies of the incoming and outgoing photons are such that the argument of the exponential is zero. We have checked that the numerical relative error in the evaluation of this integral remains always below  $10^{-6}$ . Following the same approach for the  $R_{\text{III}}$  redistribution matrix leads to a rather complicated expression. For simplicity, we take the approximation that CRD occurs in the observer's frame, for which we simply convolute the generalized profiles in equation (20) with a Gaussian function in order to account for the thermal and microturbulent velocity distribution. Thus, we substitute the Lorentzian and associated dispersion profiles appearing in

---

<sup>6</sup> We observe that the presence of an imaginary part in the redistribution function does not allow a trivial generalization to the present case of approximate methods for the evaluation of this integral, such as that proposed by Gouttebroze (1986)

Eq. (8) by the Voigt and Faraday-Voigt functions, respectively. The ensuing expression of  $[R_{\text{III}}]_Q^{K'K''}$  will be indicated as  $[R_{\text{III-CRD}}^{\text{obs}}]_Q^{K'K''}$ . The same substitutions in the generalized profiles are used in the  $\eta_i$  and  $\rho_i$  RT coefficients and in the thermal part of the line emission coefficient when transforming them into the observer's reference system.

### 3. Iterative method

In full generality, the solution of Eq. (1) for a discrete spatial grid of  $N_P$  points, for any given frequency  $\nu$  and propagation direction  $\vec{\Omega}$ , after introducing the optical depth scale  $d\tau = -\eta_I(\nu, \vec{\Omega})ds$ , can be expressed as:

$$I_i(\nu, \vec{\Omega}; n) = \sum_{j=0}^3 \sum_{m=1}^{N_P} \Lambda_{\nu, \vec{\Omega}}(n, m)_{ij} S_j(\nu, \vec{\Omega}; m) + T_i(\nu, \vec{\Omega}; n) , \quad (27)$$

where, with the letters  $n$  and  $m$ , we have explicitly indicated the dependence of the various quantities on the spatial grid points. The quantity  $S_j(\nu, \vec{\Omega}; m)$  is the so-called source function at spatial point  $m$ , defined as:

$$S_i(\nu, \vec{\Omega}; m) = \frac{\varepsilon_i(\nu, \vec{\Omega}; m)}{\eta_I(\nu, \vec{\Omega}; m)} . \quad (28)$$

Distinguishing between the line and continuum processes, the source function can be further written as:

$$S_i(\nu, \vec{\Omega}; m) = r(\nu, \vec{\Omega}; m) S_i^\ell(\nu, \vec{\Omega}; m) + (1 - r(\nu, \vec{\Omega}; m)) S_i^c(\nu; m) , \quad (29)$$

where

$$S_i^\ell(\nu, \vec{\Omega}; m) = \frac{\varepsilon_i^\ell(\nu, \vec{\Omega}; m)}{\eta_I^\ell(\nu, \vec{\Omega}; m)} , \quad (30)$$

$$S_i^c(\nu, \vec{\Omega}; m) = \frac{\varepsilon_i^c(\nu, \vec{\Omega}; m)}{\eta_I^c(\nu; m)} , \quad (31)$$

and

$$r(\nu, \vec{\Omega}; m) = \frac{\eta_I^\ell(\nu, \vec{\Omega}; m)}{\eta_I^\ell(\nu, \vec{\Omega}; m) + \eta_I^c(\nu; m)} . \quad (32)$$

The quantity  $T_i(\nu, \vec{\Omega}; n)$  is the radiation transmitted from the boundaries to point  $n$ . For given values of  $\nu$ ,  $\vec{\Omega}$ ,  $n$  and  $m$ ,  $\Lambda_{\nu, \vec{\Omega}}(n, m)_{ij}$  is a formal  $4 \times 4$  operator which depends on the propagation matrix appearing in Eq. (1). Numerically,  $\Lambda_{\nu, \vec{\Omega}}(n, m)_{ij}$  represents the contribution to  $I_i(\nu, \vec{\Omega})$  at

point  $n$  due to a source function  $S_j(\nu, \vec{\Omega})$  which is zero everywhere except at point  $m$ , where it has a value of 1. Therefore, aside from the radiation transmitted from the boundaries, all information on the generation and transfer of radiation in the atmosphere is contained in the  $\Lambda_{\nu, \vec{\Omega}}(n, m)_{ij}$  operator elements. In order to calculate these operator elements from the source function and propagation matrix, we have applied the DELOPAR formal solver (see Sect. 2). When the angle-averaged approximation for  $\mathcal{R}_{\text{II}}$  and the assumption of CRD in the observer's frame for  $\mathcal{R}_{\text{III}}$  are considered, the line emission coefficient can be expanded as

$$\varepsilon_i^\ell(\nu, \vec{\Omega}) = \sum_{K''Q''} \mathcal{T}_{Q''}^{K''}(i, \vec{\Omega}) \mathcal{E}_{Q''}^{K''}(\nu)^\ell. \quad (33)$$

A similar expansion cannot be written for the line source function since in the presence of magnetic fields of arbitrary intensity, the line part of the absorption coefficient,  $\eta_I^\ell(\nu, \vec{\Omega})$ , which appears in the denominator of the line source function (see Eq. 30), is also given by a linear combination of terms depending on the propagation direction  $\vec{\Omega}$  (see Eq. 6a). We thus write the line source function at a given frequency, direction and spatial point in the atmosphere as

$$S_i^\ell(\nu, \vec{\Omega}) = \frac{\sum_{K''Q''} \mathcal{T}_{Q''}^{K''}(i, \vec{\Omega}) \mathcal{E}_{Q''}^{K''}(\nu)^\ell}{\eta_I^\ell(\nu, \vec{\Omega})}. \quad (34)$$

Recalling the equations derived in the previous Section, it can be seen that the components  $\mathcal{E}_{Q''}^{K''}(\nu)^\ell$  are given by

$$\mathcal{E}_{Q''}^{K''}(\nu)^\ell = \mathcal{J}_{Q''}^{K''}(\nu) + k_L \frac{\epsilon'}{1 + \epsilon'} B_T(\nu_0) \Phi_0^{0K''}(J_\ell, J_u; \nu) \mathcal{D}_{0Q''}^{K''}(R_B)^*, \quad (35)$$

where  $\mathcal{J}_Q^K(\nu)$  is defined as

$$\mathcal{J}_{Q''}^{K''}(\nu) = k_L \sum_{K'Q'} (-1)^{Q'} \mathcal{D}_{Q'Q'}^{K'}(R_B) \mathcal{D}_{Q'Q''}^{K''}(R_B)^* \int_0^\infty d\nu' J_{-Q'}^{K'}(\nu') R_Q^{K'K''}(\nu', \nu; B), \quad (36)$$

with

$$R_Q^{K'K''} = [R_{\text{II-AA}}^{\text{obs}}]_Q^{K'K''} + [R_{\text{III-CRD}}^{\text{obs}}]_Q^{K'K''}. \quad (37)$$

Recalling the expression for the radiation field tensor in Eq. (5), and writing the Stokes vector in terms of the source functions as in Eq. (27), we can rewrite the  $\mathcal{J}_Q^K$  at a given spatial point as:

$$\begin{aligned} \mathcal{J}_{Q''}^{K''}(\nu; n) &= k_L \sum_{K'Q'} \int_0^\infty d\nu' R_Q^{K'K''}(\nu', \nu; n) \mathcal{D}_{Q'Q'}^{K'}(R_B) \mathcal{D}_{Q'Q''}^{K''}(R_B)^* (-1)^{Q'} \oint \frac{d\Omega'}{4\pi} \sum_{i=0}^3 \mathcal{T}_{-Q'}^{K'}(i, \vec{\Omega}') \\ &\times \left\{ \sum_{m=1}^{N_p} \sum_{j=0}^3 \Lambda_{\nu', \vec{\Omega}'}(n, m)_{ij} \left[ \frac{\sum_{K_P Q_P} \mathcal{T}_{Q_P}^{K_P}(j, \vec{\Omega}') \mathcal{E}_{Q_P}^{K_P}(\nu')^\ell}{\eta_I^\ell(\nu', \vec{\Omega}')} \right] + T_i(\nu', \vec{\Omega}'; n) \right\}, \end{aligned} \quad (38)$$

In this equation, and for the remainder of this section, the explicit dependence of  $R_Q^{K'K''}(\nu', \nu; n)$  on the magnetic field strength is no longer indicated, as this is implicitly included in the label for the spatial point  $n$ .

From the previous equations it can easily be seen how the RT problem can be solved iteratively. We start with an estimate of the radiation field tensor  $J_Q^K$  at each frequency and spatial point in the atmosphere. From this estimate, we calculate the emission coefficient  $\varepsilon_i(\nu, \vec{\Omega})$  by means of Eq. (33). From the emission coefficient, we can get new values of  $J_Q^K$  via a formal solution of the RT equations. This iterative scheme is known as the lambda iteration method which, while simple, has a very slow convergence rate in optically thick media.

For this reason, for the line part of the source function we apply the Jacobi iterative method, following Sect. 3 of Trujillo Bueno & Manso Sainz (1999). In order to simplify the notation, for the rest of this section we will omit the apex “ $\ell$ ” on the quantity  $\mathcal{E}_{Q''}^{K''}$ , being implicit that it refers to the line contribution. When applied to our problem, the Jacobi method basically consists in the following procedure. At any grid point  $n$ , the tensor  $\mathcal{J}_Q^K(\nu, n)$  is calculated through a formal solution of the RT equations, by using the values of  $\mathcal{E}_Q^K$  obtained at the end of the previous iteration, hereafter  $[\mathcal{E}_Q^K]^{\text{old}}$ , at all grid points, except at point  $n$  where the new values,  $[\mathcal{E}_Q^K]^{\text{new}}$ , are implicitly used. Within the formalism previously introduced, this reads:

$$\mathcal{J}_{Q''}^{K''}(\nu; n) = \left[ \mathcal{J}_{Q''}^{K''}(\nu; n) \right]^{\text{old}} + \int_0^\infty d\nu' \left\{ \sum_{K_P Q_P} \Lambda_{K''Q'', K_P Q_P}(\nu', \nu; n) \Delta \mathcal{E}_{Q_P}^{K_P}(\nu'; n) \right\}, \quad (39)$$

where  $\Delta \mathcal{E}_Q^K(\nu; n) = [\mathcal{E}_Q^K(\nu, \vec{\Omega}; n)]^{\text{new}} - [\mathcal{E}_Q^K(\nu, \vec{\Omega}; n)]^{\text{old}}$ , and where  $[\mathcal{J}_Q^K(\nu, \vec{\Omega}; n)]^{\text{old}}$  has been calculated according to Eq. (36), considering the radiation field tensor  $[J_Q^K]^{\text{old}}$  that is obtained from a formal solution of the RT equations, using  $[\mathcal{E}_Q^K]^{\text{old}}$  at all spatial grid points, as in the Lambda iteration method. Finally, we have defined the operator:

$$\begin{aligned} \Lambda_{K''Q'', K_P Q_P}(\nu, \nu'; n) &= k_L \sum_{K'Q'Q''} (-1)^{Q'} R_Q^{K'K''}(\nu', \nu; n) \mathcal{D}_{Q'Q'}^{K'}(R_B) \mathcal{D}_{Q''Q''}^{K''}(R_B)^* \\ &\times \oint \frac{d\vec{\Omega}'}{4\pi} \frac{r(\nu', \vec{\Omega}'; n)}{\eta_I(\nu', \vec{\Omega}'; n)^\ell} \sum_{i,j=0}^3 \Lambda_{\nu', \vec{\Omega}'}(n, n)_{ij} \mathcal{T}_{-Q'}^{K'}(i, \vec{\Omega}') \mathcal{T}_{Q_P}^{K_P}(j, \vec{\Omega}'), \end{aligned} \quad (40)$$

The correction  $\Delta \mathcal{E}_{Q''}^{K''}(\nu; n)$  is obtained by substituting Eq. (39) into Eq. (35).

Now, if the magnetic field is weak enough so that  $I \gg Q, U, V$ , then the contribution from  $\mathcal{E}_0^0$  will dominate over the others, and it will be sufficient to consider the  $\Lambda_{00,00}$  operator only

$$\begin{aligned} \Delta \mathcal{E}_0^0(\nu; n) &= \int d\nu' \Lambda_{00,00}(\nu, \nu'; n) \Delta \mathcal{E}_0^0(\nu'; n) + \mathcal{J}_0^0(\nu; n)^{\text{old}} \\ &+ k_L \frac{\epsilon'}{1 + \epsilon'} B_T(\nu_0) \Phi_0^{00}(J_\ell, J_u, \nu; n) - \mathcal{E}_0^0(\nu; n)^{\text{old}}. \end{aligned} \quad (41)$$

In this way, the Jacobi method is only applied for calculating the correction  $\Delta \mathcal{E}_0^0(\nu; n)$ , while for the rest of  $\Delta \mathcal{E}_{Q''}^{K''}(\nu; n)$  lambda iteration is used. However, when the magnetic field gets larger

and the resulting polarization fraction starts to be more significant, this approximation becomes increasingly inaccurate and the convergence rate begins to deteriorate, even producing instabilities. The first improvement that can be considered is the following: we keep applying the Jacobi method only for calculating the correction to  $\mathcal{E}_0^0$ , but we take into account the effect that polarization has on it. Recalling Eq. (38), this requires considering the contribution from the various  $\mathcal{E}_{Q_P}^{K_P}$  with  $K_P \neq 0$ ,  $Q_P \neq 0$  or, equivalently, to consider all  $\Lambda_{00,K_P Q_P}(\nu', \nu)$  in Eq. (39):

$$\begin{aligned} \Delta \mathcal{E}_0^0(\nu; n) = & \int d\nu' \sum_{K_P Q_P} \Lambda_{00,K_P Q_P}(\nu, \nu'; n) \Delta \mathcal{E}_{Q_P}^{K_P}(\nu'; n) + \mathcal{J}_0^0(\nu; n)^{\text{old}} - \mathcal{E}_0^0(\nu; n)^{\text{old}} \\ & + k_L \frac{\epsilon'}{1 + \epsilon'} B_T(\nu_0) \Phi_0^{00}(J_\ell, J_u, \nu; n) \end{aligned} \quad (42)$$

Note that this approximation is only applicable in the cases where, though contributions from  $Q, U, V$  cannot be neglected,  $|\mathcal{E}_0^0|$  is still substantially larger than other  $|\mathcal{E}_Q^K|$ . So, despite the fact that the  $\mathcal{E}_Q^K$  have a contribution from all Stokes parameters, their convergence can still be driven only by the change in  $\mathcal{E}_0^0$ . However, for larger magnetic fields, for which  $|\mathcal{E}_Q^K|$ , with  $K, Q \neq 0$ , become comparable in magnitude to  $|\mathcal{E}_0^0|$ , the Jacobi iterative scheme needs to be applied to all components, and not just to  $\mathcal{E}_0^0$ . This, on the other hand, produces a complex coupling of the various multipolar components, as well as of the various frequencies, so that the calculation of the corrections  $\Delta \mathcal{E}_{Q_P}^{K_P}(\nu; n)$  implies the solution of a huge system of equations. This is in general a formidable numerical problem, which can no longer be solved in a reasonable amount of time without resorting to suitable computational techniques. Whether one must consider all  $\Lambda_{00,K_P Q_P}$

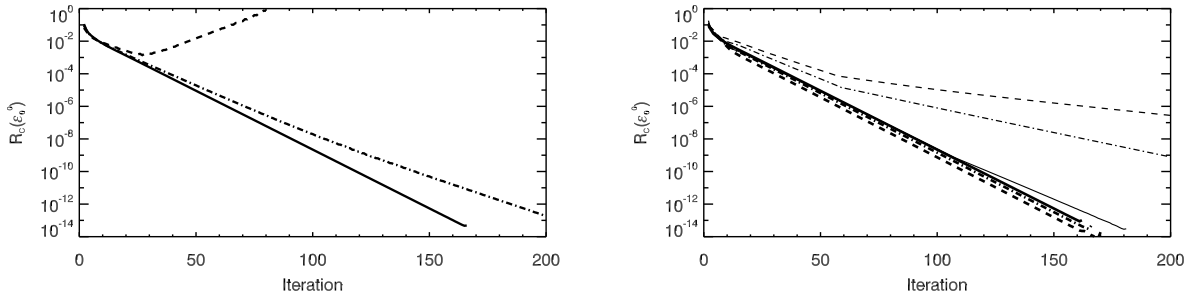


Fig. 2.— Convergence rates for  $\mathcal{E}_0^0$  for various magnetic field strengths, for a deterministic magnetic field of inclination  $\theta_B = \pi/2$  and  $\chi_B = \pi/2$ . Left: Convergence rate calculated using only the  $\Lambda_{00,00}$  operator. Right: Convergence rate calculated considering  $\Lambda_{00,K_P Q_P}$ . Results are plotted for field strengths of 0 G (thick solid line), 500 G (thick dash-dotted line), 800 G (thick dashed line), 1500 G (thin solid line), 2000 G (thin dash-dotted line), and 2500 G (thin dashed line).

operators or it is sufficient to only consider  $\Lambda_{00,00}$ , we are faced with a system of equations which we solve numerically in analogy to what is described in appendices D and E of Belluzzi & Trujillo Bueno (2014). The systems for  $\mathcal{E}_0^0$  appearing in Eq. (41) or Eq. (42) can be written, for every height

point, in a more compact form as:

$$\hat{M}\Delta\vec{\mathcal{E}}_0^0 = \vec{\mathcal{C}}, \quad (43)$$

where  $\hat{M}$  is a  $N_F \times N_F$  matrix, with  $N_F$  the number of points in the frequency grid, while  $\Delta\vec{\mathcal{E}}_0^0$  and  $\vec{\mathcal{C}}$  are vectors over the same grid. Notice that in both (41) and (42), the dependence on  $\Delta\mathcal{E}_0^0$  is the same and only  $\mathcal{C}(\nu)$  changes. When considering only  $\Lambda_{00,00}$ ,

$$\mathcal{C}(\nu; n) = \mathcal{J}_0^0(\nu; n)^{\text{old}} - \mathcal{E}_0^0(\nu; n)^{\text{old}} + k_L \frac{\epsilon'}{1 + \epsilon'} B_T(\nu_0) \Phi_0^{00}(J_\ell, J_u, \nu; n), \quad (44)$$

while when we take into account contributions from all  $\Lambda_{00,K_P Q_P}(\nu', \nu; n)$ ,  $\mathcal{C}(\nu; n)$  is calculated with additional terms related to  $\Delta\mathcal{E}_{Q''}^{K''}$ , and therefore requires much more time per iteration. Information on other methods for the transfer of spectral line polarization accounting for PRD effects can be found in Nagendra et al. (2002) and Sampoorana et al. (2008)

We have analyzed the convergence rate of our method, and its dependence on the magnetic field strength, for a deterministic field with  $\theta_B = \pi/2$  and  $\chi_B = \pi/2$ , applied to the Sr II line at 4078 Å in the atmospheric model C of Fontenla et al. (1993). The convergence rate is quantified through the maximum relative change of the  $\mathcal{E}_Q^K(\nu; n)$  quantities:

$$R_c(\mathcal{E}_Q^K) = \max \left( \frac{|\mathcal{E}_Q^K(\nu; n)^{\text{new}} - \mathcal{E}_Q^K(\nu; n)^{\text{old}}|}{|\mathcal{E}_Q^K(\nu; n)^{\text{new}}|} \right), \quad (45)$$

with the maximum evaluated over all frequencies and atmospheric heights. The variation of  $R_c(\mathcal{E}_0^0)$  with the iteration number is shown in Fig. 2 for the Sr II line at 4078 Å, where we compare the convergence rates found using only the  $\Lambda_{00,00}$  operator (left panel) and using all  $\Lambda_{00,K_P Q_P}$  (right panel). Up to around a few hundred gauss both methods perform similarly well, but as the field strength is increased up to around 500 G, the convergence rate as calculated using  $\Lambda_{00,00}$  only begins to deteriorate, and at 800 G it produces instabilities. However, when using  $\Lambda_{00,K_P Q_P}$  the convergence rate does not begin to deteriorate until around 1500 G. Then, instabilities are also encountered in this case, just above 2500 G, and in order to proceed to larger field strengths, it would be necessary to perform a computationally expensive calculation considering all  $\Lambda_{K'' Q'', K_P Q_P}$  operators. In these calculations, we have considered model C of Fontenla et al. (1993), which is composed of 70 height points. We have used a frequency grid of 183 points. The grid is finer in the line core, where the points are equally spaced, and coarser in the wings, where the separation among the points increases logarithmically. Some extra points have been added where the polarization profiles show abrupt changes (e.g., the  $Q/I$  wing peaks). As far as the integral over the propagation directions of the incoming radiation is considered, we have applied a Gauss-Legendre quadrature over the inclinations, considering 18 angles, 9 in the  $[0, \frac{\pi}{2}]$  interval and 9 in the  $[\frac{\pi}{2}, \pi]$  interval. For the azimuthal integration we used the trapezoidal method with 8 angles.



#### 4. Micro-structured magnetic field

We consider also a unimodal micro-structured magnetic field i.e., a magnetic field of a given strength and an orientation that changes over scales below the line photon's mean free path. In this case, the RT coefficients appearing in Eq (1) must be suitably averaged over the field directions:

$$\frac{d}{ds} \begin{pmatrix} I \\ Q \\ U \\ V \end{pmatrix} = \begin{pmatrix} \langle \varepsilon_I \rangle \\ \langle \varepsilon_Q \rangle \\ \langle \varepsilon_U \rangle \\ \langle \varepsilon_V \rangle \end{pmatrix} - \begin{pmatrix} \langle \eta_I \rangle & \langle \eta_Q \rangle & \langle \eta_U \rangle & \langle \eta_V \rangle \\ \langle \eta_Q \rangle & \langle \eta_I \rangle & \langle \rho_V \rangle & -\langle \rho_U \rangle \\ \langle \eta_U \rangle & -\langle \rho_V \rangle & \langle \eta_I \rangle & \langle \rho_Q \rangle \\ \langle \eta_V \rangle & \langle \rho_U \rangle & -\langle \rho_Q \rangle & \langle \eta_I \rangle \end{pmatrix} \begin{pmatrix} I \\ Q \\ U \\ V \end{pmatrix}, \quad (46)$$

where the symbol  $\langle \dots \rangle$  indicates the above-mentioned average. We shall now consider two cases: when the micro-structured field is isotropic, and when its inclination is fixed but its azimuth changes over scales smaller than the line's photon mean free path.

*a) Micro-structured isotropic field:*

In this case we need to average the RT coefficients over all inclinations  $\theta_B$  and azimuthal directions  $\chi_B$ . Observing that the dependence of the RT coefficients on the magnetic field orientation is fully contained in the rotation matrices, the problem reduces to the evaluation of the following integrals:

$$\frac{1}{4\pi} \int_0^{2\pi} d\chi_B \int_0^\pi d\theta_B \sin \theta_B \mathcal{D}_{0Q}^K(R_B)^* = \delta_{K0} \delta_{Q0}, \quad (47a)$$

$$\frac{1}{4\pi} \int_0^{2\pi} d\chi_B \int_0^\pi d\theta_B \sin \theta_B \mathcal{D}_{QQ'}^{K'}(R_B) \mathcal{D}_{QQ''}^{K''}(R_B)^* = \frac{1}{2K'+1} \delta_{K'K''} \delta_{Q'Q''}, \quad (47b)$$

where for the second equation the Weyl's theorem has been used. Note that these same averages are performed on Eqs. (41) or (42), when calculating the line part of  $\Delta \mathcal{E}_0^0$  with the Jacobi method. It has to be observed that the only nonzero coefficient in the propagation matrix is now:

$$\langle \eta_I(\nu, \vec{\Omega}) \rangle = k_L \sum_{M_\ell M_u q} \begin{pmatrix} J_u & J_\ell & 1 \\ -M_u & M_\ell & q \end{pmatrix}^2 \phi(\nu_{M_u M_\ell} - \nu). \quad (48)$$

Therefore, the four Stokes parameters will not be coupled in this case, and so the DELOPAR method shall not be required to solve the RT equation. From Eqs. (33), (30), and (35), and performing the field average described in this section, the following expression for the line emission coefficient, in the presence of an isotropic micro-structured magnetic field, is obtained:

$$\begin{aligned} \langle \varepsilon_i(\nu, \vec{\Omega})^\ell \rangle &= k_L \sum_{KQQ'} \frac{1}{2K+1} \mathcal{T}_Q^K(i, \vec{\Omega}) \int d\nu' (-1)^Q J_{-Q}^K(\nu') R_{Q'}^{K'K'}(\nu', \nu, B) \\ &\quad + k_L \frac{\epsilon'}{1+\epsilon'} \Phi_0^{00}(J_\ell, J_u, \nu) B_{\nu_0}(T). \end{aligned} \quad (49)$$

*b) Micro-structured field with fixed inclination and random azimuth:*

Fixing the inclination  $\theta_B$  and averaging over the azimuth implies the evaluation of the following

integrals:

$$\frac{1}{2\pi} \int_0^{2\pi} d\chi_B \mathcal{D}_{0Q}^K(R_B)^* = d_{00}^K(\theta_B) \delta_{Q0}, \quad (50a)$$

$$\begin{aligned} \frac{1}{2\pi} \int_0^{2\pi} d\chi_B \mathcal{D}_{QQ'}^{K'}(R_B) \mathcal{D}_{QQ''}^{K''}(R_B)^* = \\ (-1)^{Q-Q'} \sum_{\kappa} (2\kappa+1) \begin{pmatrix} K' & K'' & \kappa \\ Q & -Q & 0 \end{pmatrix} \begin{pmatrix} K' & K'' & \kappa \\ Q' & -Q'' & 0 \end{pmatrix} d_{00}^{\kappa}(\theta_b). \end{aligned} \quad (50b)$$

The RT coefficients appearing in Eq. (1), as well as the corrections  $\Delta\mathcal{E}_0^0$  that have to be calculated at each iteration, can be found following the same procedure as for the case a), but using the field averages shown in Eqs. (50) instead.

## 5. Illustrative results

In this section, we present a few illustrative applications of our RT code to resonance lines of diagnostic interest. Detailed investigations of specific spectral lines will be discussed in further publications. All following calculations have been carried out in the semi-empirical solar atmospheric model C of Fontenla et al. (1993). For the calculated linear polarization signal, we always take the reference direction for positive  $Q$  perpendicular to the Z-axis of our reference system (the local vertical). The RT problem is first solved using the RH code for the unpolarized case. The converged solution provided by this code is used as initial guess for  $J_0^0$  and  $J_0^2$  for our RT code, which we have developed following the theoretical approach described in previous sections (hereafter; the Hanle-Zeeman code). The population of the lower level, as well as the continuum RT coefficients and scattering cross section have also been obtained from the RH code. In order to accurately calculate the populations of the lower level, in the RH code we have considered a multi-level atomic model and we have considered the impact of bound-free transition via photoionization and collisional ionization processes.

For a given line, we estimate the formation height at a particular frequency as the atmospheric height at which the corresponding optical depth  $\tau$  along the line-of-sight is unity. At such height, we can estimate the fraction of coherent scattering processes (i.e., processes that are not perturbed by an elastic collision) through the so-called coherence fraction defined as:

$$\alpha = \frac{\Gamma_R + \Gamma_I}{\Gamma_R + \Gamma_I + \Gamma_E} \quad (51)$$

Our first application is for the Sr I line at 4607 Å. This photospheric resonance line is produced by a transition with  $J_u = 1$  and  $J_\ell = 0$ , and it has a Hanle critical field  $B_H = 23$  G.<sup>7</sup> For the

---

<sup>7</sup>The so-called Hanle critical field is the field strength characterizing the onset of the Hanle effect. It can be shown that  $B_H = 1.137 \cdot 10^{-7} \frac{\Gamma_R}{g_u}$ .

modeling of this line, we consider the depolarizing collisional rate  $D^{(2)}$  given in Faurobert-Scholl et al. (1995). As a second application, we consider the Sr II line at 4078 Å, a resonance line forming in the low chromosphere, with  $J_u = 3/2$  and  $J_\ell = 1/2$ . The Hanle critical field of this line is 12 G, approximately. In the modeling of this line, we neglect the depolarizing effect of elastic collisions (i.e., we set the rate  $D^{(2)} = 0$ ). For all the illustrative applications presented in this section, we consider the radiation emitted along a line-of-sight with  $\mu = 0.1$ , where  $\mu$  is the cosine of the heliocentric angle.

### 5.1. PRD calculation vs CRD limit

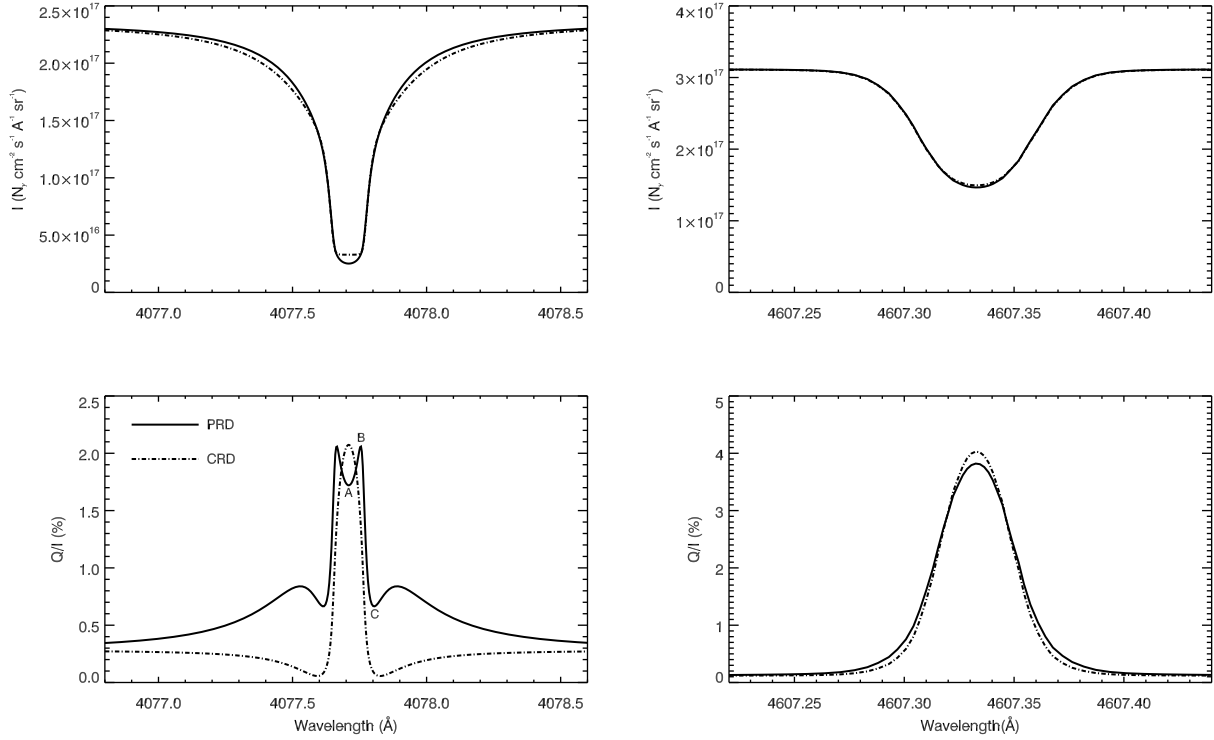


Fig. 3.— Intensity (top row) and Stokes  $Q/I$  (bottom row) profiles of the emergent radiation calculated for a line of sight with  $\mu = 0.1$  in the absence of a magnetic field, for the Sr II line at 4078 Å (left column) and for the Sr I line at 4607 Å (right column), considering the FAL-C atmospheric model. In each figure, the results for the full PRD calculation (solid line) and the results obtained in the CRD limit (dash-dotted line) are plotted. The reference direction of positive  $Q/I$  is taken perpendicular to the vertical direction.

The complex RT problem considered in this work becomes much simpler under the assumption of CRD, i.e., under the assumption that in a scattering process the frequencies of the incoming and

outgoing photons are completely uncorrelated. Therefore, it is very important to clarify when this limit can be safely applied. As mentioned before, the hypothesis of CRD is generally suitable for treating weak spectral lines, and it is a good approximation for modeling the core region of strong lines of the intensity spectrum. On the other hand, it turns out to be completely unsuitable for modeling the extended wings of strong resonance lines. In light of this, we provide now a detailed comparison between the results obtained through full PRD calculation and in the limit of CRD. In Fig 3, the emergent intensity and  $Q/I$  profiles calculated in the absence of a magnetic field are shown, for the Sr II 4078 Å line and for the Sr I 4607 Å line, comparing the full PRD calculation (solid line) to the calculation in the CRD limit (dash-dotted line). This limit has been obtained by setting the elastic collision rate  $\Gamma_E \rightarrow \infty$  while keeping all other parameters, including the  $D^{(K)}$  depolarizing collision rates, as they were. In other words, we artificially modify the branching ratios so that all scattering processes occur through the  $R_{\text{III}}$  redistribution matrix. For both lines considered, the intensity is greater at line center when using the CRD approximation than when PRD is considered. This can be qualitatively understood as follows. In the limit of CRD the scattered radiation at a given frequency depends on a weighted average of the incoming radiation over the whole line profile, and it thus takes into account that, for an absorption line, the intensity increases going from the core to the wings. On the contrary, in the limit of CS the scattered radiation is related only to the incoming radiation at that same frequency. PRD phenomena relax such coherency, relating the scattering radiation to the incoming one, but over an interval that is generally smaller than the one considered in the CRD case. This same reasoning explains why in PRD the intensity is instead larger in the wings. The same behavior can be seen when comparing PRD and CRD calculations of the fractional linear polarization  $Q/I$  profiles.

Fig. 3 clearly shows that the difference between CRD and PRD calculations is, as expected, rather small in the Sr I 4607 Å line. In particular, we expect that, once the Stokes profiles are smeared to properly account for the effects of the atmosphere’s macroturbulent velocity and of the finite spectral resolution of a typical instrument, the differences between both calculations will be negligible. The results shown for this line are in agreement with those obtained by Faurobert-Scholl (1993). Although the Sr I line at 4607 Å forms in the photosphere, where the density of neutral hydrogen (the main responsible for elastic collisions) is rather high, at the line center and for a line-of-sight with  $\mu = 0.1$ , the coherence fraction  $\alpha$  is 0.624, which means that  $R_{\text{II}}$  still represents the dominant contribution. The good agreement between PRD and CRD calculations is due to the fact that this is medium/weak spectral line without extended wings outside the Doppler core. Indeed, it has to be recalled that when Doppler redistribution is taken into account, the emergent profiles produced by  $R_{\text{II}}$  and  $R_{\text{III}}$  in the line core are very similar (see the discussion in Thomas 1957). A detailed discussion of the behavior of the two redistribution functions depending on the optical thickness of a spectral line in the core and in the wings can be found in Faurobert (1987).

The Sr II 4078 Å line forms much higher in the atmosphere, where the density of perturbers is

noticeably lower. Indeed, at the estimated formation heights for frequencies<sup>8</sup> A (4077.7091 Å), B (4077.7554 Å) and C (4077.8064 Å) for a LOS with  $\mu = 0.1$ , the coherence fractions are 0.998, 0.996 and 0.280, respectively. The contribution of  $R_{\text{II}}$  thus largely dominates in the core. In this region, however, the CRD limit still provides a rather good approximation since, as previously pointed out,  $R_{\text{II}}$  and  $R_{\text{III}}$  produce similar emergent profiles once Doppler redistribution is taken into account. Unlike the Sr I 4607 Å line, this line presents very extended wings outside the Doppler core, where the optical thickness remains considerable. In this region, the two redistribution functions have a different behavior, and they give rise to emergent polarization profiles very different from one another. It has to be noticed that the difference between the CRD and PRD  $Q/I$  profiles remains significant in the near wings also at wavelengths where the contribution of  $R_{\text{II}}$  is no longer the dominant one (see the coherence fraction at frequency point C). The three peak structure found in Stokes  $Q/I$ , with a small dip in the central one, is characteristic of coherent scattering and cannot be found in the CRD limit. Notice also that for both lines considered in the figure, there is a non-zero  $Q/I$  profile in the far wings which is produced by continuum scattering.

## 5.2. Hanle-Zeeman calculation vs Hanle limit

When the magnetic field is not too strong (e.g., outside sunspots), the splitting of the magnetic sublevels due to the Zeeman effect is generally much smaller than the Doppler width of the line. Under this circumstance, it is customary to neglect the Zeeman splitting of the energy levels in the emission and absorption profiles, as this leads to a significant simplification of the problem. Under this assumption, which is generally referred to as the weak-field approximation, the Zeeman effect is neglected by definition. In this section, we analyze the impact of using this approximation on the calculated scattering polarization profiles, when PRD phenomena are taken into account. In Fig. 4 a comparison of the full calculation and the calculation using the weak field approximation for  $Q/I$  is shown for a horizontal and transverse magnetic field, for the Sr II line at 4078 Å. Given that the magnetic field is transverse, there is no Hanle rotation, and for this reason  $U/I$  is not shown in this case. For the same reason,  $\rho_V$  is zero in this case (see the following section). At line center, the polarization in both cases is identical up to 50 G, and there is a very small discrepancy at 100 G due to a small contribution from the Zeeman effect. In the wings, however, a clear magnetic depolarization can be observed when the weak field approximation is considered. This is an artificial effect caused by the fact that we are neglecting the Zeeman splitting in the emission profile, and so the Hanle depolarization factor no longer cancels the magnetic field dependence in the wings (see Sect. 10.4 of LL04 for a more detailed discussion). It is important to note that, though the weak field approximation is reliable in the line core (as long as the conditions for its validity are met), when there are extended polarization signals in the wing - as often occurs when considering the effects of PRD on modeling strong resonant lines - one must be cautious in considering the

---

<sup>8</sup>See the lower left panel of Fig 3

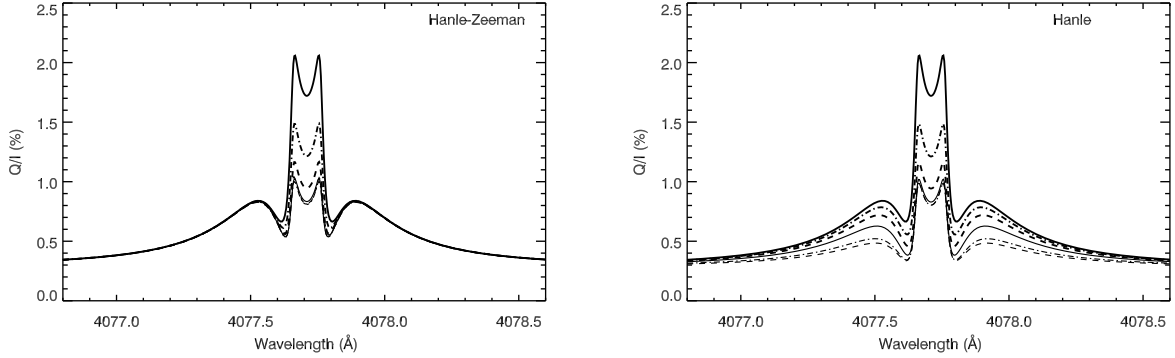


Fig. 4.— Stokes  $Q/I$  for the emergent radiation at line of sight  $\mu = 0.1$  for the Sr II line at 4078 Å in the presence of a deterministic magnetic field with  $\theta_B = \pi/2$  and  $\chi_B = \pi/2$  for various field strengths. Left panel: Full calculation. Right panel: Calculation in the weak field approximation (Hanle limit). For both cases the curves correspond to the following field strengths: 0 G (thick solid line), 5 G (thick dash-dotted line), 10 G (thick dashed line), 20 G (thin solid line), 50 G (thin dash-dotted line), 100 G (thin dashed line)

effects of the magnetic field with this approximation. The results for stronger fields are not shown because when Zeeman splitting is neglected there is no change in the polarization profiles once we have reached Hanle saturation.

### 5.3. The impact of magneto-optical effects

We consider now the emergent  $Q/I$  and  $U/I$  profiles of the Sr II line at 4078 Å, calculated for a LOS with  $\mu = 0.1$ , in the presence of a magnetic field with  $\theta_B = \pi/2$  and  $\chi_B = 0$  (i.e., a magnetic field almost longitudinal for the considered LOS). As can be observed in the left panels of Fig. 5, weak magnetic fields, even considerably below the Hanle critical field, produce a clear depolarization of the wings of the calculated  $Q/I$  profiles, and give rise to positive lobes in the wings of the  $U/I$  profiles. These effects become larger and extend further out into the line wings as the field strength grows. At first glance, this magnetic sensitivity of the line wings may appear surprising, as we know that the Hanle effect vanishes in the wings, and the contribution of the Zeeman effect to  $\varepsilon_Q$  and  $\varepsilon_U$  is expected to be negligible for these field strengths. Indeed, this magnetic sensitivity has nothing to do with such effects, but it is a magneto-optical effect, due to the term  $\rho_V$ . As it is clear from Eq. (1), this term couples  $Q$  and  $U$ , and produces a rotation of the plane of linear polarization as the radiation propagates through the atmospheric material (Faraday rotation). We recall that in the absence of lower level polarization (as in our case),  $\rho_V$  is zero unless a magnetic field with a longitudinal component is present. The coefficient  $\rho_V$  is proportional to the (antisymmetric) Faraday-Voigt profile: it is thus zero at the line center, but has very extended wings, where it can

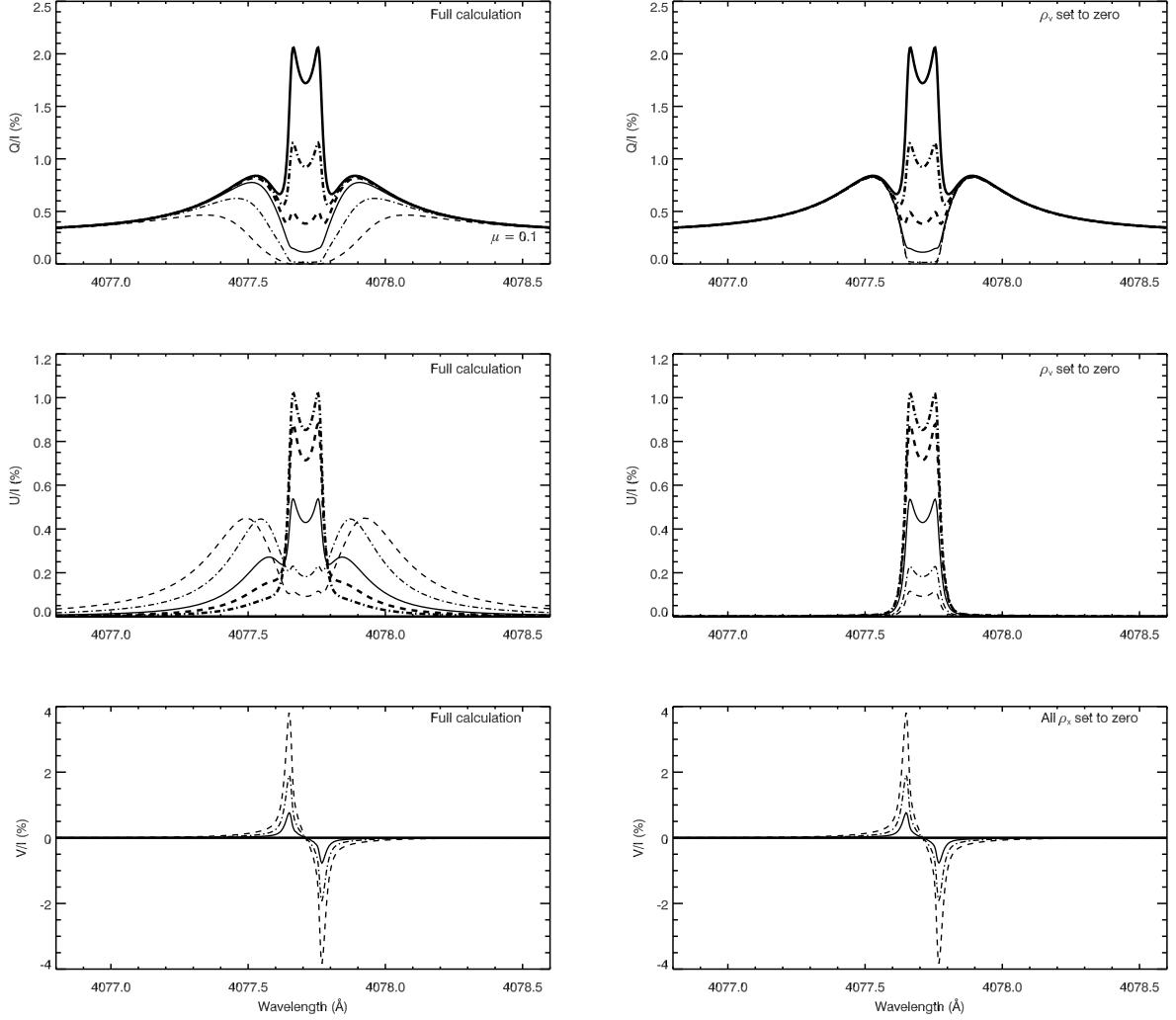


Fig. 5.— Fractional polarization  $Q/I$ ,  $U/I$  and  $V/I$  profiles of the radiation emergent at  $\mu = 0.1$  for the Sr II line at 4078 Å in the presence of a deterministic magnetic field with  $\theta_B = \pi/2$  and  $\chi_B = 0$ , for various field strengths. In the left panels the full calculations for Stokes  $Q/I$ ,  $U/I$  and  $V/I$  are presented, while in the right panels calculations are shown in which the magneto-optical term  $\rho_V$  of the propagation matrix has been neglected for  $Q/I$  and  $U/I$ , and all  $\rho_X$  terms have been neglected for  $V/I$ . The curves represent the same field strengths as in Fig. 4. However, to facilitate the visibility of the curves, for  $V/I$  the 5 G and 10 G cases are not shown.

be even larger than the absorption coefficient  $\eta_I$ . This explains why the magnetic sensitivity shown by our calculations is so clear in the line wings, while it disappears in the core of the line. Our physical interpretation of this effect is clearly supported by the results obtained by neglecting the magneto-optical effects caused by the  $\rho_V$  coefficient appearing in the propagation matrix of Eq. (1). As shown in the right panels of Fig. 5, when  $\rho_V$  is set to zero the line core signal shows exactly the same behavior as when this term is taken into account, while in the wings there is no depolarization at all in  $Q/I$ , and no signal appears in  $U/I$ . It should be observed that in our calculations we have considered an almost longitudinal field, constant throughout the whole atmosphere, a scenario that is particularly suitable for the illustration of this physical effect. It is also worth mentioning that in the Hanle-Zeeman calculation a Stokes  $V/I$  profile is produced, and it can be seen that it is not affected by the  $\rho_V$  (as can be easily deduced from Eq. 1). Moreover, for this geometry and field strength,  $\rho_Q$  and  $\rho_U$  are too weak to produce any appreciable change in the emerging circular polarization (see Fig. 5).

The magnetic sensitivity of the linear polarization in the wings of the lines, will be discussed in more detail in future publications focused on several chromospheric spectral lines.

## 6. Conclusions

In order to correctly model the scattering polarization signals of strong resonance lines in an optically thick plasma, in the presence of magnetic fields of arbitrary intensity and orientation, it is necessary to solve a complex non-LTE radiative transfer problem, taking into account the joint action of the Hanle and Zeeman effects, as well as the impact of PRD phenomena. In this work, we have considered the theoretical approach of Bommier (1997a,b), which is capable of accounting for all these physical ingredients, and we have developed and applied a series of numerical methods required for the efficient and accurate solution of the equations involved.

The resulting radiative transfer code provides a new tool for solar and stellar spectropolarimetry. It considers a two-level atomic model with an unpolarized and infinitely sharp lower level, which is suitable for investigating the magnetic sensitivity of several resonance lines of diagnostic interest such as Sr II 4078 Å, Sr I 4607 Å, or Ca I 4227 Å.

The above-mentioned theoretical approach is based on the redistribution matrix formalism. The total redistribution matrix is given by a linear combination of two terms: one describing coherent scattering processes ( $\mathcal{R}_{II}$ ) and another describing scattering processes in the limit of complete frequency redistribution ( $\mathcal{R}_{III}$ ). We have started from the expressions provided in Bommier (1997b), valid in the atomic frame, taking the quantization axis directed along the magnetic field. We have shown how to rotate them in a reference system with the quantization axis directed along an arbitrary direction, and how to transform them from the atomic rest frame into the frame of the observer. The expressions corresponding to the case in which a magnetic field that changes its direction over scales smaller than the line photon's mean free path have also been studied.



We have presented illustrative results for the Sr I photospheric line at 4607 Å and for the Sr II chromospheric line at 4078 Å, and in forthcoming publications we will describe in detail other interesting applications to the  $k$  line of Mg II at 2795 Å and to the Ca I line at 4227 Å. The main results are the following:

- *The impact of PRD phenomena.* Calculations accounting for the effects of PRD have been compared to those in the CRD limit, in order to quantitatively evaluate the suitability of this approximation. In photospheric lines without significant wings such as Sr I 4607 Å, we can confirm that the CRD limit is a very good approximation for modeling the intensity and scattering polarization. Nevertheless for strong chromospheric lines, with extended wings outside the Doppler core, such as Sr II 4078 Å the impact of PRD phenomena is very significant, especially in the near wings. The resulting scattering polarization profiles show extended wings and complex multi-peak structures. Such profiles cannot be found in the limit of CRD, which however keeps representing a quite good approximation for modeling the line-center amplitude of both intensity and scattering polarization signals. While in the atomic reference frame coherent scattering effects play an important role also in the line center, in the observer's frame the effects of Doppler redistribution cause the CRD approximation to be suitable to estimate the polarization at the line center. But in the near wings the effects of PRD need to be taken into account, for both the intensity and the emergent scattering polarization.
- *The weak-field approximation in the general PRD case.* In another application to the Sr II 4078 Å line we compared the results obtained when applying the weak field approximation with the results of our Hanle-Zeeman calculation. While in the line core the resulting scattering polarization signals agree, in the wings we find that the results for the weak-field approximation become inaccurate, since artificial signals are found when neglecting the Zeeman splitting in the absorption and emission profiles.
- *Magneto-optical effects in the general PRD case.* Furthermore, we have found that in strong resonance lines for which PRD effects produce sizable  $Q/I$  wing signals, such as that of Sr II at 4078 Å, a novel physical mechanism operates that creates  $U/I$  wing signals and introduces a very interesting magnetic sensitivity in the wings of the  $Q/I$  and  $U/I$  profiles. This magnetic sensitivity has nothing to do with the Hanle effect, nor with the Zeeman effect in emission. Instead, we conclude that it is caused by magneto-optical effects; in particular, by the coupling between Stokes  $Q$  and  $U$  due to the  $\rho_V$  term of the propagation matrix as the radiation propagates through the magnetized solar atmosphere.

We would like to thank the anonymous referee for insightful and helpful comments. We are also grateful to Tanausú del Pino Alemán (HAO) for several scientific discussions during the development of this work that were very helpful to refine the numerical method presented here for solving the PRD radiative transfer problem for arbitrary magnetic fields. Likewise, we are grateful

to Egidio Landi Degl’Innocenti (University of Firenze) for illuminating discussions on the applied theory of spectral line polarization. Financial support by the Spanish Ministry of Economy and Competitiveness through projects AYA2014-55078-P and AYA2014-60476-P is gratefully acknowledged. E. Alsina Ballester also wishes to acknowledge the Fundación La Caixa for financing his Ph.D. grant.

## REFERENCES

- Belluzzi, L., & Trujillo Bueno, J. 2014, *A&A*, 564, A16
- Bianda, M., Stenflo, J. O., & Solanki, S. K. 1998, *A&A*, 337, 565
- Bommier, V. 1997a, *A&A*, 328, 706
- . 1997b, *A&A*, 328, 726
- Casini, R., & Landi Degl’Innocenti, E. 2007, in *Plasma Polarization Spectroscopy*, ed. T. Fujimoto & A. Iwamae, 247
- Casini, R., Landi Degl’Innocenti, M., Manso Sainz, R., Landi Degl’Innocenti, E., & Landolfi, M. 2014, *ApJ*, 791, 94
- Faurobert, M. 1987, *A&A*, 178, 269
- . 1988, *A&A*, 194, 268
- Faurobert-Scholl, M. 1993, *A&A*, 268, 765
- Faurobert-Scholl, M., Feautrier, N., Machefert, F., Petrovay, K., & Spielfiedel, A. 1995, *A&A*, 298, 289
- Fontenla, J. M., Avrett, E. H., & Loeser, R. 1993, *ApJ*, 406, 319
- Gouttebroze, P. 1986, *A&A*, 160, 195
- Landi Degl’Innocenti, E., Landi Degl’Innoncenti, M., & Landolfi, M. 1997, in *THEMIS Forum: Science with THEMIS*, ed. N. Mein & S. Sahal-Bréchet, Observatoire de Paris, 59–77
- Landi Degl’Innocenti, E., & Landolfi, M. 2004, *Polarization in Spectral Lines* (Klumer Academic Publishers)
- Mihalas, D. 1978, *Stellar atmospheres /2nd edition/*
- Nagendra, K. N., Frisch, H., & Faurobert, M. 2002, *A&A*, 395, 305
- Rees, D. E., & Saliba, G. J. 1982, *A&A*, 115, 1

- Sampoorna, M. 2011, A&A, 532, A52
- Sampoorna, M., Nagendra, K. N., & Stenflo, J. O. 2008, ApJ, 679, 889
- Sowmya, K., Nagendra, K. N., Sampoorna, M., & Stenflo, J. O. 2014, ApJ, 793, 71
- . 2015, ApJ, 814, 127
- Stenflo, J., ed. 1994, Astrophysics and Space Science Library, Vol. 189, Solar Magnetic Fields: Polarized Radiation Diagnostics
- Thomas, R. N. 1957, ApJ, 125, 260
- Trujillo Bueno, J. 2003, in Astronomical Society of the Pacific Conference Series, Vol. 288, Stellar Atmosphere Modeling, ed. I. Hubeny, D. Mihalas, & K. Werner, 551
- Trujillo Bueno, J., & Manso Sainz, R. 1999, ApJ, 516, 436
- Trujillo Bueno, J., Shchukina, N., & Asensio Ramos, A. 2004, Nature, 430, 326